

# Silicon Micromachined Fiber-Optic Accelerometer for Downhole Seismic Measurement

Non-member Kaoru Hirata (Tohoku University)

Member Hiroaki Niitsuma (Tohoku University)

Member Masayoshi Esashi (Tohoku University)

The fabrication and characterization of a fiber-optic micro accelerometer for downhole seismic measurement is described. This sensor consists of a Fabry-Perot interferometer using a half-mirror at the end of an optical fiber and a total reflection mirror on a silicon mass suspended with thin beams. When acceleration is applied to the sensor, the intensity of the reflected light is modulated interferometrically according to the displacement of the silicon mass.

The sensor is fabricated by using silicon micromachining and hence is small sized (6.6 mm in diameter and 11 mm in height) and cost effective. By reason of the small size and the low cost, it is possible to install many sensors in a micro borehole. Since the sensor has not active devices like transistors, it can stand in harsh environment i.e. high temperature. The fabricated sensor has the frequency range from DC to 300 Hz, the maximum detectable acceleration of 0.27g and the dynamic range of 36 dB.

Keywords: Optical Fiber, Accelerometer, Fabry-Perot Interferometer, Downhole Seismic Measurement

## 1. INTRODUCTION

In Tohoku University, the development of various kinds of microsensors for downhole measurement has been made since 1993 [1]. Micromachining is the technology for fabricating three-dimensional microstructures. Using this technology, it is possible to fabricate a large number of precise microstructures on a silicon wafer with low cost [2].

Micro accelerometers have been developed for seismic detection. If the micro accelerometers are realized, it is easy to install many seismic sensors in a micro borehole or in casing annulus of a borehole. A fiber-optic micro accelerometer has been developed since 1993 (Nouta et al.) [3]. The sensor is fabricated by using silicon micromachining and hence is small sized and cost effective. Since the sensor has not active devices like transistors, it can stand in harsh environment i.e. high temperature. We have already reported the concept of the fiber-optic micro accelerometer for downhole seismic measurement [4]. This report describes the fabrication and characterization of the sensor.

## 2. THE PRINCIPLE OF DETECTING ACCELERATION

Figure 1 shows the principle of detecting acceleration in the fiber-optic micro accelerometer. The sensor consists of a Fabry-Perot interferometer using a half mirror at the end of an optical fiber and a total reflection mirror placed on the silicon mass. The detected light intensity from the sensor is expressed as follows,

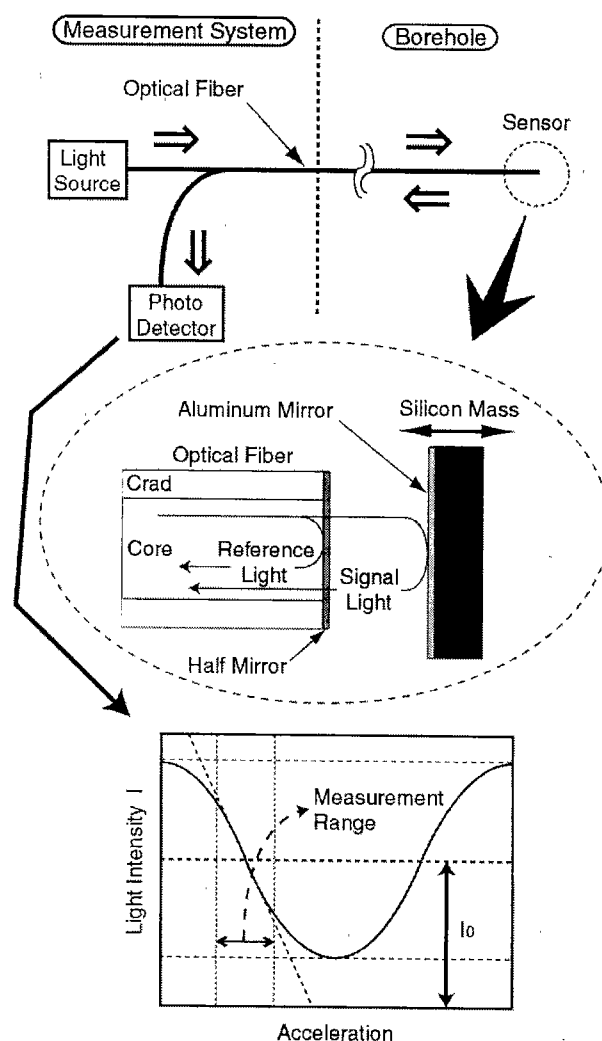


Fig.1. Principle of detecting acceleration

$$I = [I_0] + [\text{Modulated Signal}]$$

$$= [A_1^2 + A_2^2] + \left[ 2A_1A_2 \cos\left(\frac{4\pi B}{\lambda} \cos(\omega_s t) + \frac{4\pi d}{\lambda}\right) \right], \quad (1)$$

where  $I_0$  is the mean light intensity,  $A_1, A_2$  are the amplitudes of the reflected light from the end of the optical fiber and the silicon mass,  $\lambda$  is the light wavelength,  $B$  is the displacement of the silicon mass,  $d$  is the gap between the end of the optical fiber and the inner surface of the silicon mass,  $\omega_s$  is the angular frequency of the silicon mass movement, and  $t$  is time. The modulated signal component extracted from Eq.1 is expressed as follows,

$$I' = -4A_1A_2J_1\left(\frac{4\pi B}{\lambda}\right)\sin\left(\frac{4\pi d}{\lambda}\right)\cos(\omega_s t), \quad (2)$$

where  $J_1(x)$  is the 1st Bessel function. Around  $x=0$   $J_1(x)$  is approximately proportional to  $x$  and hence the modulated signal  $I'$  is proportional to the mass displacement  $B$ .

In order to maximize the modulated signal  $I'$  following condition is required.

$$\frac{4\pi d}{\lambda} = \frac{\pi}{2} + n\pi \quad (n=0,1,2,\dots), \quad (3)$$

In order to satisfy Eq.3, the wavelength of the light source i.e. semiconductor laser diode (LD) could be adjusted within a few nano-meter by changing the temperature.

The ratio between  $I_0$  and the amplitude of the modulated signal in Eq.1 is defined as "visibility". The larger the visibility the higher the sensor sensitivity. The maximum visibility  $\gamma_m$  is represented in Eq.4,

$$\gamma_m = \frac{[\text{Modulated Signal}]}{[I_0]}$$

$$= \frac{2A_1A_2}{A_1^2 + A_2^2}$$

$$= \frac{2r_1t_1^2f}{r_1^2 + t_1^4f^2}, \quad (4)$$

where  $r_1$  and  $t_1$  are amplitude reflectivity and amplitude transmittance at the end of the optical fiber and  $f$  is the fraction of the reflected light into the fiber core. The amplitude reflectivity at the end of the silicon mass is 1. These components are shown in Fig.1. When the reflectivity of the half mirror at the fiber end is optimized i.e.  $r_1 = t_1^2 f$ , large  $\gamma_m$  is obtained [4].

### 3. DESIGN

Figure 2 shows the schematic diagram of the fiber-optic micro accelerometer of which size is 6.6 mm in diameter and 11 mm in height. The silicon mass is suspended with thin beams from a frame on both front and backsides in order to suppress cross axis sensitivity. The silicon frame is fixed at the end of the glass micro capillary in which a single-mode optical fiber is inserted. The gap for the optical interferometer is made between the end of the optical fiber and the aluminum mirror on the silicon mass. The opposite side of the silicon is covered with a Pyrex glass plate. Multi-mode optical fiber could not be used because of its phase divergence.

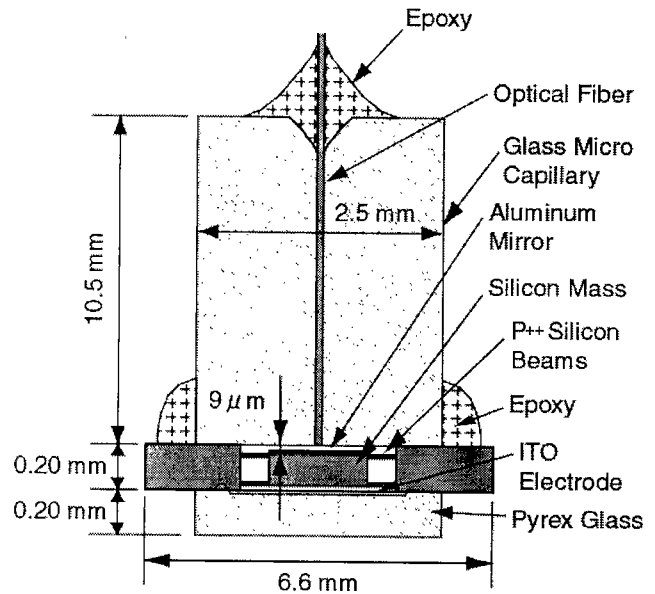


Fig.2. Schematic diagram of the fiber-optic micro accelerometer

The maximum detectable acceleration  $a_m$ , the resonant frequency  $f_n$  and damping ratio  $\xi$  are determined by the following equations respectively,

$$a_m \propto \frac{1}{[\text{Sensitivity}]} \propto \frac{k}{m}, \quad (5)$$

$$f_n = \frac{1}{2\pi} \sqrt{\frac{k}{m}}, \quad (6)$$

$$\xi = \frac{0.21\mu S^2}{d^3 \sqrt{mk}}, \quad (7)$$

where  $k$  is spring constant,  $m$  is mass,  $\mu$  is viscosity of air,  $S$  is area of the silicon mass. The specifications were required considering the use for the downhole seismic

measurement [5]. The sensor design is listed in Table.1.

Table.1. The sensor design

Whole Size		6.6 × 6.6 × 10.9 [mm]
Silicon Mass	Area	0.43 [mm <sup>2</sup> ]
	Thickness	180 [μm]
	Weight	0.18 [mg]
Beams	Number	8
	Length	510 [μm]
	Width	20 [μm]
	Thickness	4.3 [μm]
Spring Constant		10.5 [N/m] (by 8)
The Gap between two Mirrors		9 [μm]
Maximum Detectable Acceleration	$a_m$	0.33 [g]
Resonant Frequency	$f_n$	1216 [Hz]
Damping Ratio	$\xi$	0.70

#### 4. FABRICATION

The fabrication process of the micromachined silicon and the assembly process are described in the following (Fig.3). The vertical etching through the silicon wafer was made using ICP-RIE (Inductively Coupled Plasma – Reactive Ion Etching). The thin beams made of highly doped P<sup>++</sup> layer were formed by undercutting the silicon with selective wet etching using EPW (Ethylenediamine-Pyrocatechol-Water)

as an etchant [6]. The packaging of the sensor was achieved by anodically bonding the micromachined silicon to a Pyrex glass and fixing the silicon-glass structure to the glass micro capillary (Nippon Electrical Glass) by Epoxy.

- ① Both side polished and (100) oriented silicon wafer 200 μm in thickness was used.
- ② 9 μm gap was formed by anisotropic wet etching using TMAH (Tetra-Methyl-Ammonium-Hydroxide).
- ③ Boron was diffused in order to form 4.3 μm thick highly doped P<sup>++</sup> layer.
- ④ SiO<sub>2</sub> stoppers were formed by plasma TEOS-CVD (TEOS: Tetra-EthOxy-Silane).
- ⑤ Vertical etching through the silicon wafer was made by ICP-RIE with SiO<sub>2</sub> as a mask. The SiO<sub>2</sub> was deposited by plasma TEOS-CVD.
- ⑥ The beams were formed with selective wet etching using EPW as an etchant.
- ⑦ SiO<sub>2</sub> mask was etched to the extent that the SiO<sub>2</sub> stoppers remained.
- ⑧ Aluminum was evaporated though a mask for the reflected mirror.
- ⑨ Indium-Tin-Oxide (ITO) was sputtered on the Pyrex glass. The Pyrex glass was bonded anodically to the micromachined silicon. The electrically conductive ITO film was required to avoid an undesirable bonding of the silicon mass to the glass by electrical shielding.

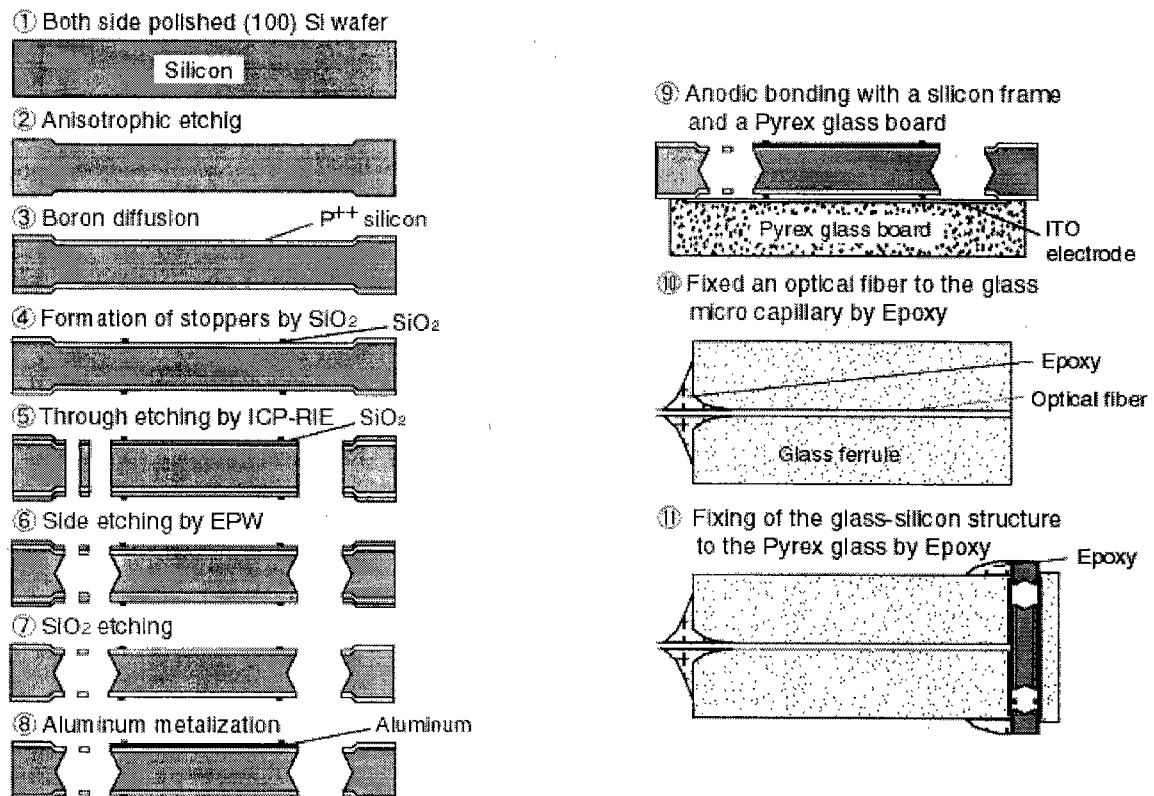


Fig.3. Fabrication and assembly process of the sensor

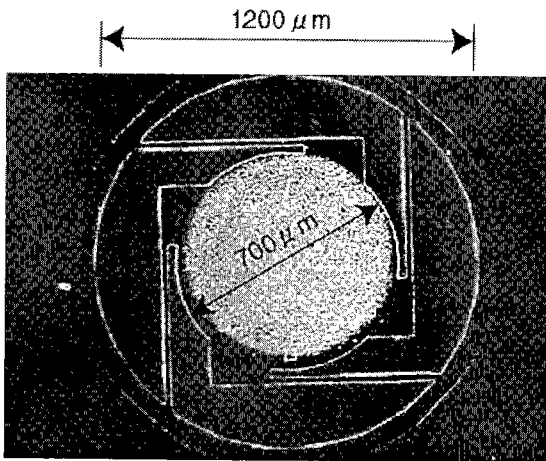


Fig.4. Photograph of the micromachined silicon

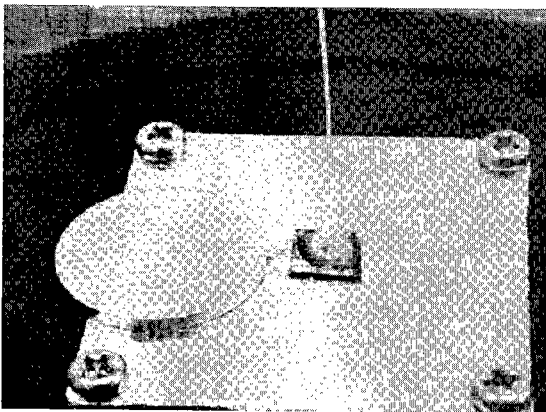


Fig.5. Photograph of the packaged sensor mounted on a vibration exciter

- ⑩ Optical fiber was inserted and fixed to a glass micro capillary by Epoxy.
- ⑪ The silicon-glass structure was fixed to the glass micro capillary by Epoxy.

Figure 4 show the photographs of the micromachined silicon structure. The mass is suspended with thin beams as shown in the photograph in order to release the residual stress which originates in the highly doped P<sup>++</sup> layer. Figure 5 is the photograph of the packaged sensor that is mounted on a vibration exciter.

## 5. CHARACTERISTICS

Figure 6 shows a measurement setup for static characteristics of the sensor, in which the LD (LN7301 Panasonic) and the light detector (Q8347 ADVANTEST) was used. The wavelength of the LD is approximately 1300nm. In this setup, the wavelength of the LD was adjusted by changing the temperature in order to satisfy the condition of Eq.3. The sensor response against the tilt angle of the sensor was measured. Figure 7 shows the static characteristics of the sensor. The result shown in Fig.7 was

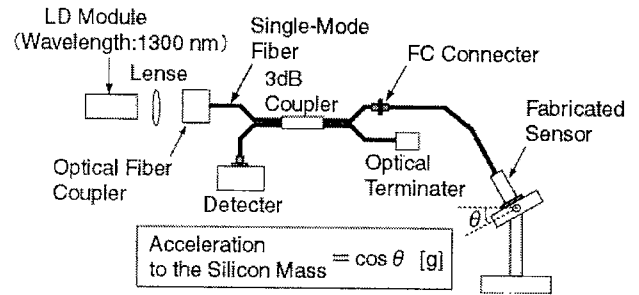


Fig.6. The measurement setup for static characteristics

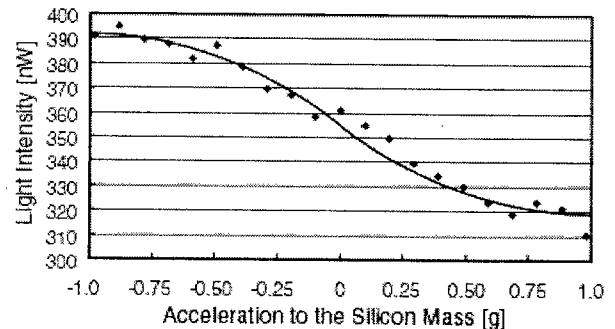


Fig.7. Static characteristics of the sensor

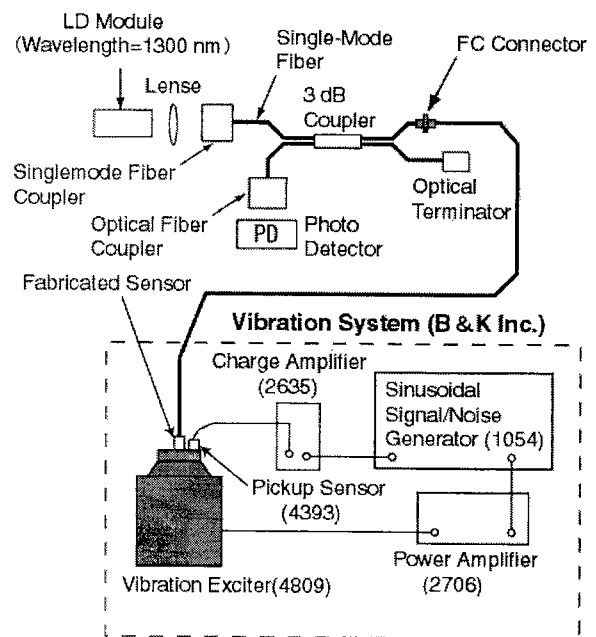


Fig.8. Measurement system for dynamic characteristics

reproducible and the influence of the bending and the vibration of the optical fiber was negligible. The theoretical displacement of the silicon mass is 336nm under the static acceleration of  $\pm 1g$ . The displacement corresponds approximately to a quarter of the wavelength of the light source. Figure 7 represented the good agreement with the theoretical displacement, that is, it saturates around  $\pm 1g$ . Although the experimental result didn't completely correspond with the theoretical curve, it seems that the silicon mass didn't necessarily displace horizontally to the

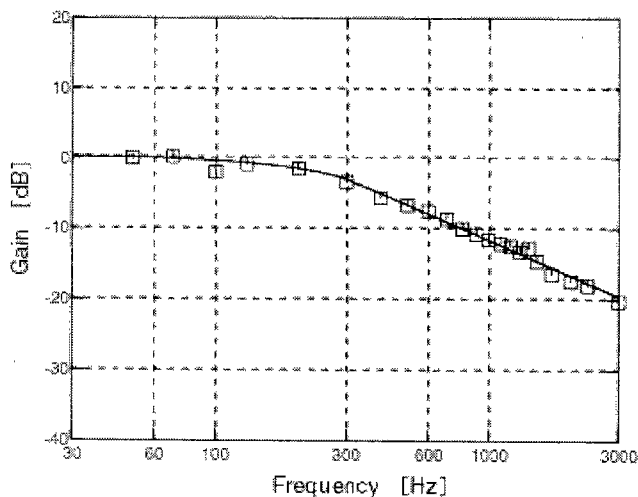


Fig.9. Frequency characteristics

direction of the acceleration that was determined by the tilt angle of the sensor.

Figure 8 shows a measurement system for the dynamic characteristics of the sensor. The dynamic characteristics were measured by fixing the fabricated sensor on a vibration exciter (4809 B&K). The photodiode (G5832-02 HAMAMATSU PHOTONICS) was used to detect the light intensity. Figure 9 shows the frequency characteristics of the fabricated sensor. The fabricated sensor has a frequency range from DC to 300Hz. The estimated damping ratio is 2.0, because the gain is -12 dB at the theoretical resonant frequency (1200 Hz). Damping ratio is larger than that designed, because the gap between the Pyrex glass plate and the silicon mass could not be well controlled by reason of the distortion of the Pyrex glass plate caused during anodic bonding. To solve the problem, it seemed to be effective to use the thick Pyrex glass plate for reducing the distortion [7]. The dynamic range of the fabricated sensor is characterized as shown in Fig.10. The maximum and minimum detectable acceleration is 0.27 g and 0.004 g respectively and the dynamic range is 36 dB. The maximum detectable acceleration measured satisfies the required specification. However, the minimum detectable acceleration that is equal to the noise level is too large to detect the seismic signal. To lower the minimum detectable acceleration it is required to increase the light intensity to the detector and to improve the detector. The reflectivity at the fiber end was not optimized in the fabricated sensor because the fiber end didn't have a half mirror but its natural reflectivity. Furthermore it is required to minimize the optical loss at the connector and so on or to increase the light intensity of the LD to achieve higher sensitivity.

## 6. CONCLUSION

We have developed the fiber-optic micro accelerometer that has endurance in harsh environment for downhole use.

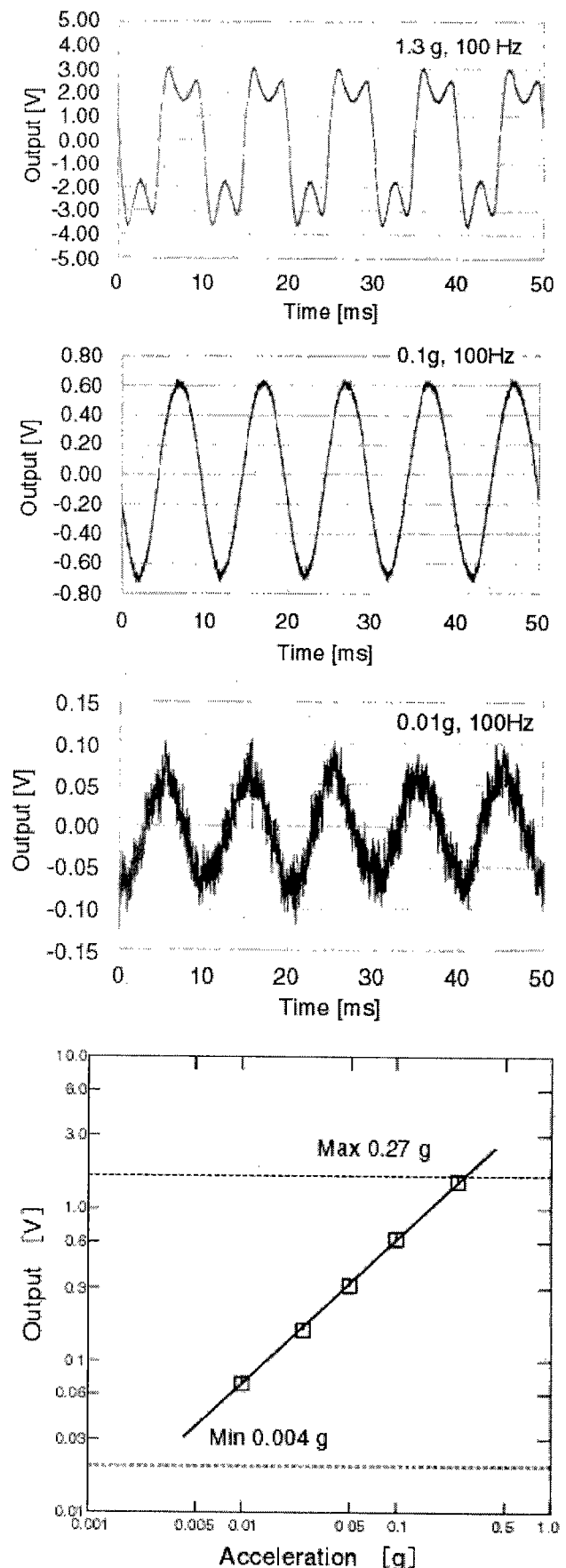


Fig.10. Dynamic range of the sensor

The fabricated sensor has the frequency range from DC to 300HZ, the maximum detectable acceleration of 0.27g, and the dynamic range of 36 dB. The future work is to lower the minimum detectable acceleration and to package the sensor for the use of downhole seismic measurement.

## ACKNOWLEDGEMENT

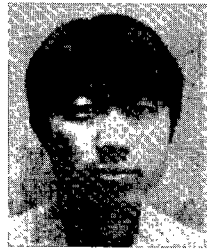
This work was performed in Venture Business Laboratory in Tohoku University being supported by The Japanese Ministry of Education, Science and Culture under Grant-in-aid No.09305068. We express our gratitude to colleagues who helped us in experiments.

(Manuscript received August 26, 1999, revised March 21, 2000)

## REFERENCES

- [1] H. Niitsuma, "Concept of Subsurface Micro-sensing", Proceedings of the 96th SEGJ Conference, Tokyo, pp.33-34, 1997. (In Japanese)
- [2] M. Esashi, "Micromachining and Sensors", The journal of the Institute of Electrical Engineers of Japan, 110, pp.203-210, 1990. (In Japanese)
- [3] T. Nouta, "Development of an Optical Interference-Type Sensor for Subsurface Microseismic Measurement by Using Micromachining Technique", M.S. thesis, Tohoku University, 1995. (In Japanese)
- [4] K. Hirata, H. Niitsuma, M. Esashi, "Development of an Optical Interference-Type Micro Accelerometer for Subsurface Microseismic Measurement", Proceedings of the 97th SEGJ Conference, Sapporo, pp.165-168, 1997. (In Japanese)
- [5] S. Nagashima, "Development and Calibration of Downhole Triaxial AE Detectors for Subsurface and Civil Engineering AE Measurements", Progress in Acoustic Emission 6, 1, 1, pp.407-413, 1992.
- [6] G. Lim, S. Baek and M. Esashi, "A New Bulk-Micro Machining Process Using Deep RIE and Wet Etching", Proceedings of the Institute of Electrical Engineering, Tokyo, PS-97-32, pp.59-62, 1997. (In Japanese)
- [7] Y. Shoji, K. Minami, M. Esashi, "Glass-Silicon Anodic Bonding for the Reduction of Structural Distortion", T. IEE Japan, vol.115-A, No.12, pp.1208-1213, 1995.

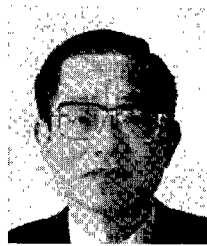
### Kaoru Hirata



mass flow controller.

(non-member) received the B.S. degree in resources engineering from and M.S. degree in Geoscience and Technology from Tohoku University, Sendai in 1997 and 1999, respectively. He is currently pursuing the D.E. degree in Mechatronics and Precision Engineering. His current research involves the development of a micro

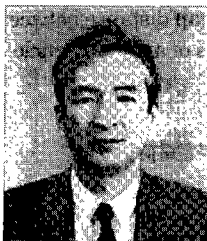
### Hiroaki Niitsuma



interests include subsurface instrumentation. Professor Niitsuma is a representative of the international collaboration program "Establishment of new mapping/imaging technologies for advanced energy extraction from deep geothermal reservoirs -MTC Project-" funded by NEDO and MESCC. He is a director of the SPWLA Japan Chapter, SEGJ and MMIJ, and a Councilor of the Geothermal Research Society.

(member) received the B.S., M.S. and D.E. degrees in Electrical Communication Engineering from Tohoku University, Sendai in 1970, 1972 and 1975, respectively. He is currently a professor at department of Geoscience and Technology, graduate school of engineering, Tohoku University. His current research

### Masayoshi Esashi



fabricated with micro machining.

(member) received the B.S., M.S. and D.E. degrees in Electronic Engineering from Tohoku University, Sendai in 1971, 1973 and 1976, respectively. He is currently a professor at New Industry Creation Hatchery Center, Tohoku University. His current research interests include micro sensors and integrated micro systems